

Anisotropic Elastoplastic Behavior Formulation and Analysis of the Instability in the Large Deformations: A Numerical Modeling Study in Forming Processes

Khalid Zhani^{1*}, Ahmed Chenaoui¹, Nabih Saadi¹

¹ Department of Physics, Mechanical and Civil Engineering Laboratory, Faculty of Sciences and Technology, University Abdelmalek Essaadi, Tangier, Morocco

* Corresponding author's e-mail: k.ezhani@gmail.com

ABSTRACT

This study focuses on investigating the elastoplastic behavior and predicting plastic instabilities that occur during the large deformations in the metal and alloy forming process. The behavior was modelled using a phenomenological model with velocity-independent plasticity. This model takes into account the various physical phenomena encountered in the cold forming of metal sheets, in particular the initial anisotropy of the material and work hardening. The resulting constitutive equations were written in an incremental form, and the behavior law was introduced in a three-dimensional kinematic framework based on a particular writing of the gradient tensor of the deformations and gradient of the velocities in the form of an upper triangular matrix. The results demonstrate that the observed behavior is contingent upon the selection of a rotating reference frame. The impact of the selection of a rotating reference frame on the response of the behavior law is considerable. However, for loads with minimal rotation, this influence is negligible. When analysing the instabilities, we tested various prediction to understand the conditions that lead to deformations and to compare these different instability criteria. As a case study, the forming limits curves were analyzed.

Keywords: Cordebois's criterion, Instability elastoplastic behavior, phenomenological model, Rice's criterion, rotating reference frame.

INTRODUCTION

Some research projects have been devoted to controlling the industrial processes involved in shaping metals and alloys, because of their industrial and economic interests. However, during these shaping operations, phenomena such as localization of deformations and significant plastic instabilities occur, which makes it necessary to know the critical deformations and the location of these plastic deformations to characterise the formability of various metals, as well as the mechanisms limiting their formability and causing their fracture.

Several approaches exist to predict and overcome these challenges, In theory, to overcome these problems and predict the occurrence of

these phenomena [1, 2], some authors use the approach of forming limit curves (FLC) introduced by Keeler and Goodwin [3, 4], and Hill [5] was one of the first to propose a prediction model based on a phenomenological description of the material's behavior by adopting a rigid isotropic plastic model for the prediction of the left part of the FLC, Marciniak and Kuczynski [6] introduced the concept of initial imperfection. These phenomenological models remained limited in that they did not take into account certain essential physical characteristics of the material's behavior, such as the initial and induced textures and other microstructural parameters. To overcome these limitations, others are adopting advanced micromechanical modelling [7]; Panicaud et al. [8, 9] to analyse the impact of the material

on the microstructure. Modelling is employed to analyse the impact of microstructural aspects on ductility and to establish relationships between microstructure and formability. While others rely on numerical simulation using the finite element method as a powerful tool for the virtual design of various industrial sheet metal processes [10, 11]. The modelling of the mechanical behavior of metals in large elastoplastic deformations has been extensively studied, and the conceptual difficulties concerning the formulation of elastoplasticity in large transformations have been sufficiently mastered in [12-15] using the rotating reference frame formalism. Firstly, the precise description of the behavior law of the material making up the sheet and its influence on the response to particular stresses remains an open subject and is the subject of much research work. Secondly, the selection of an appropriate criterion for predicting plastic instabilities, which can manifest in various forms (such as necking or shear bands) and lead to defects during forming operations, in this context, in order to address these issues, we have employed a common general framework for the formulation of the behavior of materials, which allows for the reproduction of elastoplastic behavior in finite transformations. This framework was introduced in a three-dimensional kinematics framework based on particular writing of deformation gradient and velocity gradient tensors by an upper triangular matrix [16, 17] that was developed to facilitate numerical resolution and integration and to enable the integration of two Cordebois-Ladeveze and Rice [18-20] plastic instability prediction criteria in the context of large deformations. The first criterion is based on the principle of virtual powers, while the second is based on deformation heterogeneities, using a bifurcation approach. The basic model utilised is that of phenomenological plasticity, which was introduced in a large elastoplastic transformation case involving either isotropic or anisotropic materials [18]. In this case, plasticity is assumed to be either associated with or not associated with strain-hardening, for which we assume that the elasticity is relatively small.

In particular, the use of non-associated plasticity has enabled this work to overcome the normality problem encountered by Hill (in the rigid case) and thus to predict critical deformations in positive deformation domains.

CONTRIBUTION

In this context, the work presented here can be evaluated as follows: The behavior was formulated according to three choices of rotating referential, and the Rice and Cordebois-Ladvez criterion was expressed according to Sidoroff's constitutive phenomenological model [21, 22], based on Mandel's work. It is sufficient to state that the present study tests the validity of the approach proposed by Rice and Cordebois and the influence of the choice of a rotating reference frame. Especially, this work addresses the limitations of previous models by employing a comprehensive framework for material behavior in large elastoplastic deformations. A novel formulation using a three-dimensional kinematics framework allows for integrating Cordebois-Ladeveze and Rice criteria for predicting plastic instabilities. This approach overcomes the normality problem encountered in earlier models, providing a more accurate prediction of critical deformations.

The study's novelty lies in its three-dimensional kinematic framework, using a specific upper triangular matrix form that enhances numerical resolution and integration speed. However, limitations remain, particularly in accurately predicting elastic behavior and initial yield points. An improved elasticity criterion is necessary for better modeling under various stress states. While the current algorithm is not optimal, it achieves results in under 10 minutes. The authors acknowledge the potential for improvement in more complex scenarios. The results of this theoretical model demonstrate a positive correlation with empirical and experiment data, indicating the effectiveness of the model in simulating the mechanical response of the material.

Table 1. Conventions, notations, and acronyms

\cdot^e	: the elastic part of \cdot
\cdot^p	: the plastic part of \cdot
\cdot^s	: the symmetric part of \cdot
\cdot^T	: transpose of tensor \cdot
$\cdot \cdot$: time derivative of \cdot
\cdot^{-1}	: inverse of \cdot
F	: the deformation gradient tensor
Q	: the rotation tensor
L	: the strain velocity gradient tensor
V	: the elastic strain tensor
Ω	: the spin
W	: the antisymmetric part of L
τ	: the stresses tensor
\mathcal{E}	: the shortening tensor
D	: the strain rates of deformation tensor
\cdot^{ani}	: the anisotropic matrix
$\cdot \cdot$: the double contraction product between \cdot and \cdot
Note that the stress (MPa) values shown in the figures are divided by Young's Modulus E (GPa).	

MATERIALS AND METHODS

Formulation of anisotropic elastoplasticity in a rotating frame of reference

The rotating frame of reference represents the optimal framework for modelling anisotropic elastoplasticity in large deformations [23, 24]. The anisotropic elastoplastic material is considered an elastic medium with respect to an isoclinic configuration \bar{C} in accordance with Mandel's terminology [12, 25]. Its orientation is defined by a "directing trihedron" (Mandel trihedron), which is linked to the material element. This leads to a multiplicative decomposition of the deformation gradient F , with the plastic deformation gradient part \bar{F}^P and the elastic part F^e which rotates (Q) and distorts the material element (V^e):

$$F = F^e \bar{F}^P = V^e Q \bar{F}^P \quad (1)$$

This rotating reference frame is defined by the rotation Q , which, according to Mandel [12, 25], postulates the existence of a privileged directing trihedron linked to the material element. Let us suppose that \bar{m}_i and \vec{m}_i represent the privileged trihedron in two different configurations: (i) the initial configuration C_0 and the isocline \bar{C}^p , and (ii) the released intermediate configuration C_t^e , which was deduced by elastic deformation from the current configuration C_t . In this case, the rotation Q can be defined as:

$$Q = \bar{m}_i \otimes \vec{m}_j = Q_{ij} \vec{e}_i \otimes \vec{m}_j \quad (2)$$

In order to ensure the law of objectivity and material frame indifference, as outlined by Dogui [23] and Sidoroff [24], the rotation must be transformed into a rotation defined by q ($F \rightarrow F' = qF$), which can then be expressed as a rotation Q' :

$$Q \rightarrow Q' = qQ \quad (3)$$

Rotation defines the movement of a rigid solid. The strain velocity gradient tensor is expressed in the deformed configuration as follows C_t by:

$$L = \dot{F}F^{-1} = \dot{V}^e V^{e-1} + V^e \Omega V^{e-1} + V^e \bar{L}^P V^{e-1} \quad (4)$$

Where \bar{L}^P represents the Lagrangian plastic strain velocity gradient tensor, defined in the isoclinic configuration by:

$$\bar{L}^P = \dot{\bar{F}}^P \bar{F}^{P-1} \quad (5)$$

From a practical point of view, for metals, the elastic distortion is often negligible:

$$V^e = I + \varepsilon^e \text{ and } \|\varepsilon^e\| \ll 1 \quad (6)$$

In this context, the identity tensor is represented by I , while the symmetric elastic strain tensor is represented by ε^e . For the purposes of this analysis, the second term and any higher powers of ε^e and $\dot{\varepsilon}^e$ are neglected.

The relationship (4) can then be simplified to:

$$L = (\dot{\varepsilon}^e - \Omega \varepsilon^e + \varepsilon^e \Omega) + \Omega + L^P \quad (7a)$$

Or L^P is the gradient tensor of Eulerian plastic strain velocity which is defined by:

$$L^P = Q \bar{L}^P Q^T \quad (7b)$$

By breaking it down into a symmetrical part $D = L^S$ and antisymmetric $W = L^A$, we get:

$$L = D + W \quad (7c)$$

$$D = L^S = D^e + D^P \quad (7d)$$

$$W = L^A = W^P + \Omega \quad (7e)$$

Relation (7d) represents the equation for deformation and D is the strain rates of deformation. While relation (7e) represents the rate of rotation of the reference frame linked to the deformed configuration C_t .

The tensors D^e , D^P and W^P are defined by:

$$D^e = \dot{\varepsilon}^e - \Omega \varepsilon^e + \varepsilon^e \Omega \quad (8a)$$

$$D^P = L^{PS} \quad (8b)$$

$$W^P = L^{PA} \quad (8c)$$

In the isoclinic configuration, \bar{L} is defined by:

$$\bar{L} = \dot{\bar{F}}\bar{F}^{-1} = Q^T L Q = \dot{\varepsilon}^e + \bar{\Omega} + \bar{L}^P \quad (9)$$

Or $\bar{\Omega}$ is the spin of the rotating reference frame in the isoclinic configuration is defined by:

$$\bar{\Omega} = Q^T \Omega Q = Q^T \dot{Q} \quad (10)$$

The symmetrical part of the \bar{L} defines the Lagrangian total rate of deformation tensor \bar{D} , for its antisymmetric part \bar{W} , it represents the total Lagrangian rotation velocity tensor. These tensors are defined in the isoclinic configuration by:

$$\bar{D} = \bar{L}^S = Q^T D Q = \bar{D}^e + \bar{D}^P \quad (11)$$

$$\bar{W} = \bar{L}^A = Q^T W Q = \bar{\Omega} + \bar{W}^P \quad (12)$$

and:

$$\bar{D}^e = Q^T D^e Q = \dot{\varepsilon}^e \quad (13a)$$

$$\bar{D}^P = \bar{L}^{PS} = Q^T D^P Q \quad (13b)$$

$$\bar{W}^P = \bar{L}^{PA} = Q^T W^P Q \quad (13c)$$

Equations of the anisotropic elastoplastic model

In this case, the anisotropic model equations are approached similarly to the isotropic model used in [26], and the constitutive laws are introduced in the rotating reference frame rather than the Eulerian reference frame.

Elastic law

In this type of structure, the law of elasticity is considered in the rotating reference frame defined by the double contraction product between the elasticity matrix and strain tensor:

$$\dot{\bar{\tau}} = \bar{C} : \dot{\bar{\epsilon}} \quad (14)$$

\bar{C} is the elasticity matrix defined in the isoclinic configuration.

This law can be written in the Eulerian configuration with the objective derivative by:

$$\check{\tau} = C : \check{\epsilon} \quad (15)$$

with:

$$C_{ijkl} = Q_{ip} Q_{jq} Q_{kr} Q_{ls} \bar{C}_{pqrs} \quad (16)$$

In the case of isotropic elasticity, the tensor C is expressed as a function of Young's modulus and Poisson's ratio.

Plastic flow

The associated flow law that follows provides the plastic deformation tensor, as per Sidoroff [21] and Dafalias [13]:

$$\bar{D}^p = \dot{\lambda} \frac{\partial \bar{f}}{\partial \bar{\tau}} = \dot{\lambda} \bar{N} \quad (17)$$

\bar{N} represents the plastic flow direction, it is normal to the charged surface and it is defined by the potential \bar{f} in the isoclinic configuration \bar{C} .

λ is the plastic multiplier, which is determined by the charge-discharge criteria.

$$\begin{cases} \bar{f}(\bar{\tau}, p) = \bar{\Sigma}(\bar{\tau}) - R(p) \\ \dot{\lambda} \geq 0 \\ \dot{\bar{f}} = 0 \end{cases} \quad (18)$$

Or $\bar{\Sigma}$ is the equivalent stresses, a function of the stresses $\bar{\tau}$ defining the shape of the loading surface in stress space (elastic domain). Finally, R represents the size of the loading surface, linked to the isotropic strain-hardening of the material anisotropic, the most commonly used basic model is that of Hill [27] defined by:

$$\bar{\Sigma} = \sqrt{\frac{3}{2} \bar{\tau}^D : \bar{H} : \bar{\tau}^D} \quad (19)$$

Or $\bar{\tau}^D$ and τ^D are the deviatoric part of the Kirchhoff stress $\bar{\tau}$ and τ , and \bar{H} the Hill anisotropy matrix, where:

$$\begin{aligned} \bar{\Sigma}^{1/2} = & F * (\bar{\tau}_{22} - \bar{\tau}_{33})^2 + G * (\bar{\tau}_{33} - \bar{\tau}_{11})^2 \\ & + \mathcal{H} * (\bar{\tau}_{11} - \bar{\tau}_{22})^2 + 2L\bar{\tau}_{12} \\ & + 2M\bar{\tau}_{13} + 2N\bar{\tau}_{23} \end{aligned}$$

The Hill coefficients are given in Table 2.

In this case, the direction of flow is defined by:

$$\bar{N} = \frac{\partial \bar{\Sigma}}{\partial \bar{\tau}} = \sqrt{\frac{3}{2}} \bar{H} : \frac{\bar{\tau}^D}{\bar{\Sigma}} \quad (20)$$

Hardening law

The following paragraphs will examine the isotropic hardening law, which is defined by Swift's law:

$$R(p) = h(\bar{\epsilon}^p + \epsilon_0)^n \quad (21)$$

The term n represents the hardening exponent, whereas the parameter h denotes the material constant.

The cumulative plastic strain is defined by:

$$\bar{\epsilon}^p = \sqrt{\frac{3}{2} |\bar{D}^p|} \quad (22)$$

Tangent module

Calculating the tangent matrix involves finding the relationship between the Kirchhoff stresses ratio $\check{\tau}$ and the rate of deformation \bar{D} . According to expressions (14) and (15), we can write:

$$\dot{\check{\tau}} = \bar{C} : (\bar{D} - \bar{D}^p) \quad (23)$$

Using (17) we have:

$$\check{\tau} = C : \left(D - \dot{\lambda} \bar{N} \right) \quad (24)$$

To calculate $\dot{\lambda}$ we use the consistency condition $\dot{f}(\tau, p) = 0$ and we obtain:

$$\dot{\lambda} = \frac{\bar{N} : \bar{C} : \bar{D}}{R'(p) + \bar{N} : \bar{C} : \bar{N}} \quad (25)$$

By introducing the relation (25) into (24), we obtain:

$$\dot{\check{\tau}} = \bar{C} : \left(\bar{D} - \frac{\bar{N} : \bar{C} : \bar{D}}{R'(p) + \bar{N} : \bar{C} : \bar{N}} \bar{N} \right) \quad (26)$$

Hence the incremental law in the isoclinic configuration:

$$\dot{\check{\tau}} = \bar{\mathcal{A}}^{\text{ani}} : \bar{D} \quad (27)$$

The matrix $\bar{\mathcal{A}}^{\text{ani}}$ designates the tangent modulus representative of the elastoplastic behavior law linking, on the one hand, the Kirchhoff stresses tensor and, on the other hand, the strain rate.

Writing (27) the behaviour law has the advantage of avoiding the decomposition into elastic and inelastic deformation. However, there remains the choice of objective derivatives from the multitude proposed in the literature, which is difficult and requires physical justification.

- Jaumann’s case.

For this case, we take:

$$\Omega = \dot{Q}Q^T = W \quad (28)$$

W is the strain rate, which may be written as follows:

$$W = \frac{1}{2}(L - L^T) \quad (29)$$

According to definitions (29), (14) and (23):

$$\dot{\tau} = \mathcal{A}^{ani}; L - \tau W + W\tau \quad (30)$$

or:

$$\dot{\tau} = \mathcal{A}^{ani}; L + \frac{1}{2}\{-\tau L + \tau L^T + L\tau - L^T\tau\} \quad (31)$$

This can be written as:

$$\dot{\tau} = \mathcal{A}^{ep}; L \quad (32)$$

\mathcal{A}^{ep} being a tangent matrix representative of the behaviour.

It is the incremental constitutive law linking the time derivative ($\dot{\tau} = \mathcal{A}^{ep}; L$) to the strain velocity gradient tensor L.

- Dafalias case.

In this case, we have:

$$\Omega = \dot{Q}Q^T = W - \omega \quad (33)$$

and:

$$w = 2a_1(m_2 D^p m_3)^A + 2a_2(m_3 D^p m_1)^A + 2a_3(m_1 D^p m_2)^A$$

$$w = w^{23} + w^{31} + w^{12} \quad (34)$$

If we consider the first term, we have:

$$w^{23} = 2a_1(m_2 D^p m_3)^A;$$

$$w_{ij}^{23} = 2a_1 m_{ip}^2 G_{pqkl} D_{kl} m_{qj}^3 \quad (35)$$

either:

$$w_{ij}^{23} = \Omega_{ijkl}^1 D_{kl} \quad (36)$$

with:

$$\Omega_{ijkl}^1 = 2a_1 m_{ip}^2 G_{pqkl} D_{kl} m_{qj}^3 \quad (37)$$

Similarly for the others, we obtain:

$$\Omega_{ijkl}^2 = 2a_2 m_{ip}^3 G_{pqkl} D_{kl} m_{qj}^1 \quad (38)$$

$$\Omega_{ijkl}^3 = 2a_3 m_{ip}^1 G_{pqkl} D_{kl} m_{qj}^2 \quad (39)$$

The final result is:

$$w = \Omega; D \text{ and } \Omega = \Omega^1 + \Omega^2 + \Omega^3 \quad (40)$$

or:

$$\dot{\tau} = A; L + w\tau - \tau w \quad (41)$$

Hence (41) is written:

$$\dot{\tau} = (A + A^2); L \quad (42)$$

or:

$$A_{ijkl}^2 = \Omega_{imkl} \tau_{mj} - \tau_{im} \Omega_{mjkl} \quad (43)$$

In general, relationship (49) can be rewritten as:

$$\dot{\tau} = [(A^{ani} + A^1 + A^2)]; L = A^{ep}; L \quad (44)$$

$$A_{ijkl}^1 = \frac{1}{2}(-\tau_{ik} \delta_{jl} + \tau_{il} \delta_{kj} + \tau_{ik} \delta_{jl} - \tau_{ik} \delta_{jl}) \quad (45)$$

$$A_{ijkl}^2 = \Omega_{imkl} \tau_{mj} - \tau_{im} \Omega_{mjkl}$$

$$A^{ep} = A^{ani} + A^1 + A^2 \quad (46)$$

RESULTS AND DISCUSSIONS

This section delves into the analysis of the results, encompassing: first, the analysis of constraints based on the calculations of stresses and shear strains; second, an analysis of instability, followed by a discussion of the results. The equation systems are numerically solved using the fourth-order Runge-Kutta method. The programming is written in the Matlab environment, and the instability is predicted by a test of Rice’s [28] and Cordebois’s criterion.

In this section and during the mechanical tests studied, we demonstrate the change in behavior in relation to the reference frames chosen, as well as the effect of the rotation induced for the prediction criterion used on the (FLC).

The numerical results illustrated for the simulation of the anisotropic elastoplastic behavior independent of the rotation spin were obtained in the case of a power-type hardening law defined above. To demonstrate the feasibility of the calculation, the material parameters were chosen from a case study by Habracken et al. [29], where the Hill coefficients were given by Lankford. The material parameters [29] were fitted to the Lankford coefficients, their values are shown in Table 2.

Constraints analysis

Within the framework of the kinematics presented above, we numerically integrated the various equations obtained for the different tests: simple tensile, simple shear, and plane compression. The integration of the systems is resolved

Table 2. Material parameters (Aluminum alloy)

Parameter	Value
M, N, L	2.5091
F	0.5395
G	0.5526
H	1.4474
Initial critical value τ_0	0.01
Material constant h/E	0.007
Hardening exponent m	0.24
Young's Modulus E (GPa)	70
Poisson's coefficient	0.33

Note: The stress values shown in the figures are divided by E.

using an explicit or implicit formalism depending on the degree of precision required.

For these distinct types of tests, we conducted an analysis of the behaviour in order to ascertain the significance of the choice of rotating reference frame for the formulation of the behaviour law and the impact of strain hardening as well as the influence of induced anisotropy, by implementing the evolution of the rotation angles. It should be noted that in some studies, the effect of the orientation of the rolling angle was studied to reduce the anisotropy and reduce the average microhardness for Al-Cu and AlCuV alloys [30].

- Simple tensile and biaxial test cases.

Figures 1 and 2 show the effect of the choice of a rotating frame of reference on the evolution of τ_{11} and Π_{11} as a function of the ϵ in the anisotropic

case for a simple tensile test and a biaxial test. In both cases, the choice of Green-Naghdi and Jaumann reference frames yielded no discernible influence on the two tests for the stress τ_{11} . Contrary to the force Π_{11} where the evolution is the same at the beginning until the 4% of deformation, after this threshold, the evolution becomes significant between the two tests for the two cases of the chosen reference frame. From these curves, we note that the hardening order obtained is qualitatively consistent with the results of experimental tests [31] in the case of less rigid materials. This shows the importance of the hardening effect, a result confirmed by Zhani et al. [17] in the case of Channel-die.

- Simple shear test case.

The figures below shows the evolution of stresses τ_{11} (Fig. 2) and τ_{12} as a function of slip in the case of a shear test for different rotating reference frames shear test in the anisotropic case for Jaumann, Green-Naghdi rotation and Dafalias (Fig. 3).

In the case of the simple shear test, for Green-Naghdi we note that the evolution is significant compared with that of Dafalias and less important than that of Jaumann (Figure 3). It can be seen that the choice of reference frame has a significant effect on strain hardening. In the case of the choice of the Green-Naghdi reference frame, we note that the evolution is greater than that of Dafalias and less than that of Jaumann (Figure 3). We can see that the choice of reference frame has an important effect on the strain hardening. We can see that the evolution in the case of Green-Naghdi is more important than that of Dafalias and less important than that of Jaumann.

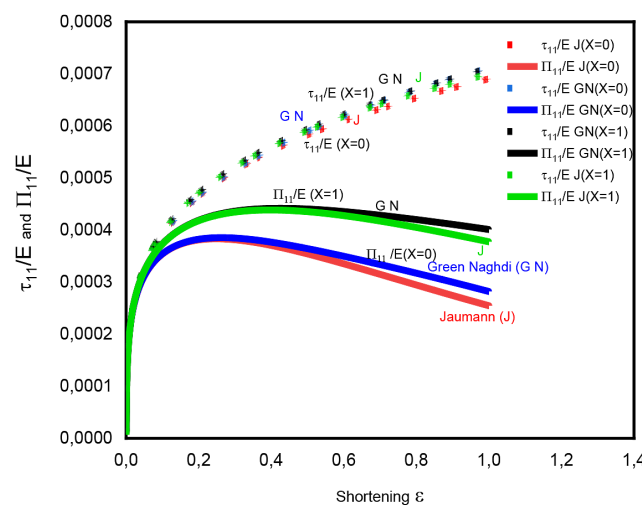


Figure 1. Stresses τ_{11}/E and Π_{11}/E as a function of shortening ϵ (calculated for simple tensile and biaxial expansion)

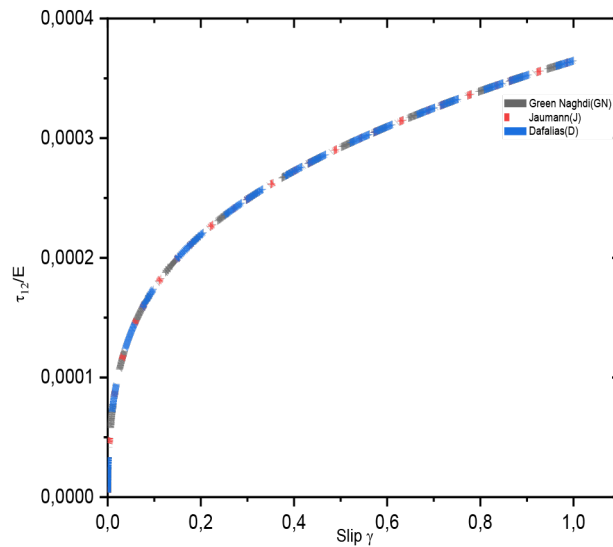


Figure 2. Stresses τ_{12}/E as a function of slip γ (calculated for a simple shear)

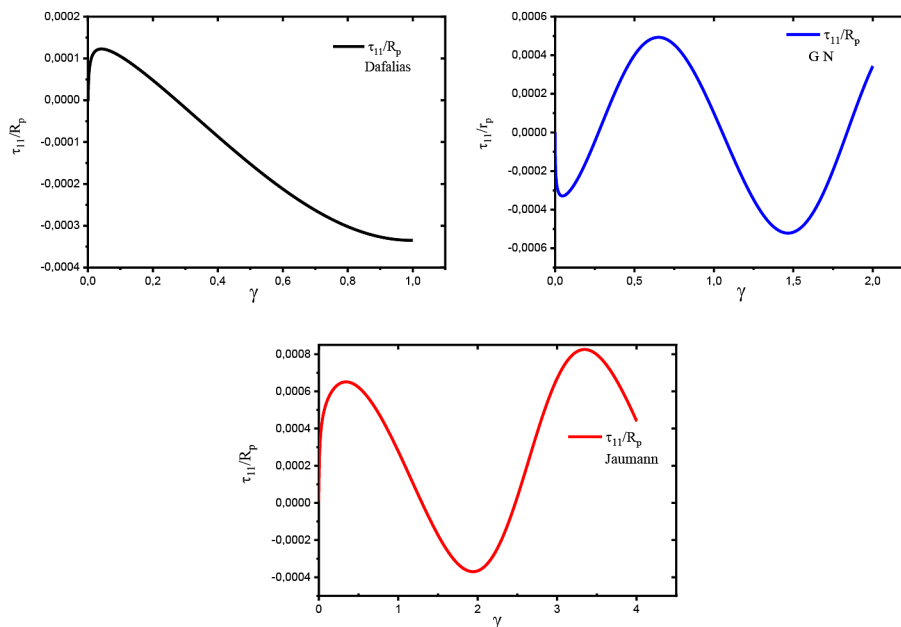


Figure 3. Stresses τ_{11}/R_p as a function of slip γ (calculated for a simple shear)

- Channel-die test case.

In the anisotropic case, Figure 4 shows the effect of the choice of rotating reference frame on the evolution of the normal stress σ_{33}/E as a function of the shortening ϵ in the case of a plane compression test, this case was widely studied by Zhani et al. [17]. We note that the evolution in the Jaumann case is more important than that of the Geen-Naghdi. in this case and for the normal stress, the hardening phenomenon is qualitatively consistent with experimental investigations in the case of single crystals [31], particularly for the less hard materials.

Rotation analysis

The results of the simulations presented in the Figures 5 and 6 illustrate the influence of the rotating reference frame on the induced anisotropy and were obtained for the various mechanical tests. They show that the choice of frame of reference has a significant influence on anisotropy and behavior, and therefore on the time taken for plastic instabilities to appear. This effect is very significant in the case of self-rotation and is influenced by the evolution of hardening.

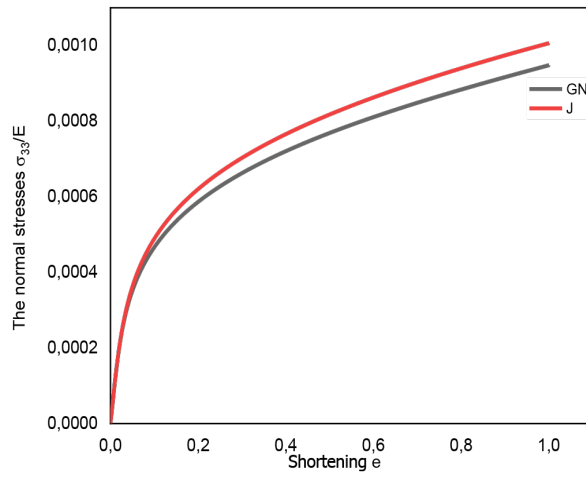


Figure 4. Normal stresses σ_{33}/E as a function of shortening ϵ (calculated for a channel-die compression)

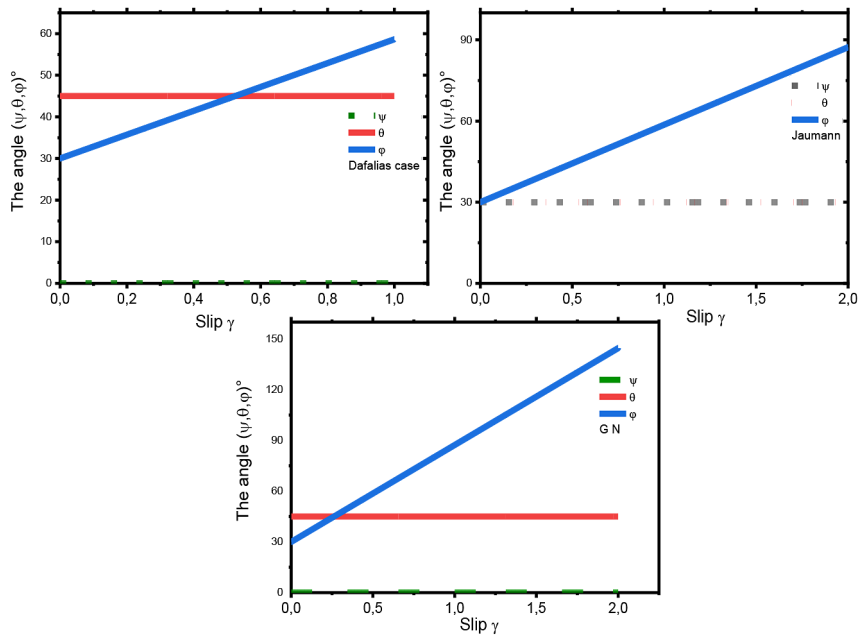


Figure 5. Angle (ψ, θ, ϕ) as a function of the slip γ (calculated for a shear test)

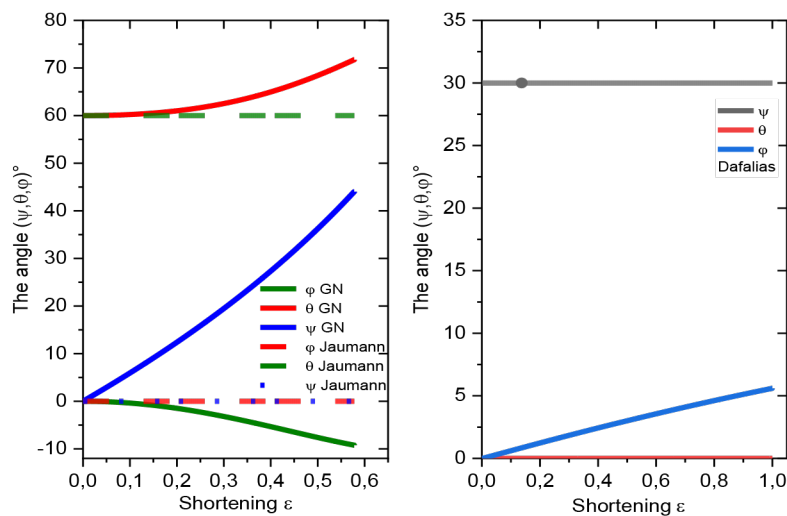


Figure 6. Angle (ψ, θ, ϕ) as a function of the shortening ϵ (calculated for a simple tensile test)

Instability analysis

Figures 7 show that the initial orientation has an influence on the FLCs and the instability prediction criterion. In general, we can draw the conclusion that the simulations demonstrate the ability of FLDs to predict instability and that the ultimate outcome may rely more on the constitutive model that is employed as well as the instability approach that is chosen. Effect of choice of rotating reference frame on constraints, for Rice's Criterion and Cordebois's Criterion (Figure 8).

We can conclude from the results above that, for loads generating large rotations (e.g. simple sliding), the choice of rotating reference frame has a substantial impact on the behavior law's reaction. However, for loads with little rotation (e.g. off-axis tensile) this influence is negligible, especially if the deformations are not very large.

CONCLUSIONS

In conclusion, the results of the numerical simulations indicate that the selection of a rotating reference frame is an essential element in the formulation of a behaviour. In the case of the Green-Naghdi reference frame, it can be observed that the evolution is greater than that of Dafalias and less than that of Jaumann.

The influence of the rotating frame of reference on mechanical stresses for elastoplastic behavior has been studied. It has been found that the effect of the choice of frame of reference is slight in some cases, generally during stress-strain analysis. However, it is significant in others, such as the case of large sliding. However, when studying instabilities, it is necessary to consider rotations and the influence of the choice of a rotating frame of reference. The results were corroborated in

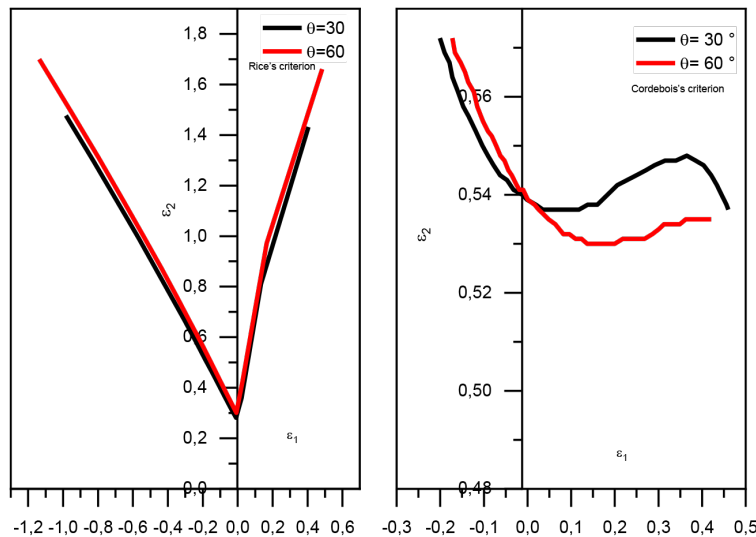


Figure 7. The minor strain ϵ_2 as a function of the major strain ϵ_1 (calculated for a simple tensile test for Rice's and Cordebois's criterion)

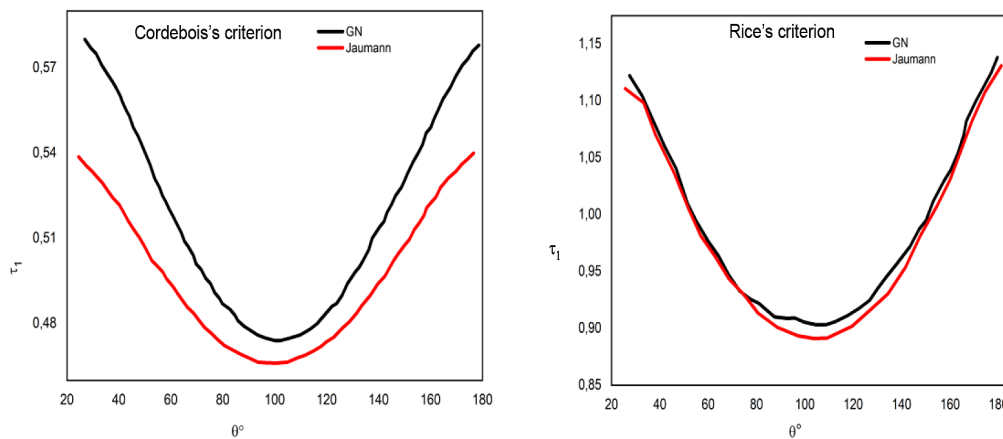


Figure 8. The stresses τ_1 as a function of the angle θ (calculated for a simple tensile test for Cordebois's and Rice's criterion)

two-dimensional kinematics. The formulation of large strains requires the use of multiple tensors, but the introduction of a material rotation frame, where the deformation tensor is represented by an upper triangular matrix, greatly simplifies the calculations.

It is noted that the results obtained in this work constitute a means of comparing, theoretically and numerically, various formulations in large elastoplastic deformations. Furthermore, these results can be obtained by simulation in a finite element code, and they will be verified and validated by experimental results. Furthermore, this work has confirmed the findings of the microscopic mechanical analysis conducted at the single-crystal scale, which forms part of the microstructural study of the material's behavior. It has also revealed the influence of the orientation of single-crystal grains on the emergence and location of plastic instabilities.

REFERENCES

1. Crisfield MA. Non-linear finite element analysis of solids and structures. Chichester, Wiley; 1991.
2. Lee EH. Elastic-plastic deformations at finite strains. *ASME Journal of Applied mechanics*, 1970, 37(1): 243-244. DOI: <https://doi.org/10.1115/1.3408472>
3. Keeler SP. Determination of forming limits in automotive stampings. *SAE Transactions*, 1966,74: 1–9. <https://doi.org/10.4271/650535>
4. Goodwin. Application of the strain analysis to steel metal forming in press shop. *la Metallurgia Italiana*, 1968; (8): 767-72.
5. Hill RT. On discontinuous plastic states, with special reference to localized necking in thin sheets. *Journal of the Mechanics and Physics of Solids*. 1952; 1(1): 19-30. [https://doi.org/10.1016/0022-5096\(52\)90003-3](https://doi.org/10.1016/0022-5096(52)90003-3)
6. Marciniak Z, Kuczynski K. Limit strains in processes of stretch-forming sheet metal. *Int J Mech Sci*. 1967; 9: 609-20. DOI: [https://doi.org/10.1016/0020-7403\(67\)90066-5](https://doi.org/10.1016/0020-7403(67)90066-5).
7. Akpama HK, Ben Bettaieb M, Abed-Meraim F. Prediction of plastic instability in sheet metals during forming processes using the loss of ellipticity approach. *Latin American Journal of Solids and Structures*. 2017; 14: 1816-1836. <https://doi.org/10.1590/1679-78253544>.
8. Panicaud B, Saanouni K, Baczmanski A, François M, Cauvin L, Le Joncour L. Theoretical modelling of ductile damage in duplex stainless steels - comparison between two micro-mechanical elastoplastic approaches. *Computational Materials Science*. 2011; 50: 1908-1916.
9. Panicaud B, Le Joncour L, Hfaiedh N, Saanouni K. Micromechanical polycrystalline damage-plasticity modeling for metal forming processes. Chapter 28 of the Section VI Damage Mechanics in Metal Forming. Voyiadjis G, editor. "Handbook of Damage Mechanics: Nano to Macro Scale for Materials and Structures". 2015; 2(NB): 816-75.
10. Akpama HK, Ben Bettaieb M, Abed-Meraim F. Prediction of Localized Necking Based on Crystal Plasticity: Comparison of Bifurcation and Imperfection Approaches. *KEM*. 2016; 716: 779-89. <https://doi.org/10.4028/www.scientific.net/kem.716.779>.
11. Szala, M., Winiarski, G., Bulzak, T. A., Wójcik, Ł. (2022). Microstructure and Hardness of Cold Forged 42CrMo4 Steel Hollow Component with the Outer Flange. *Advances in Science and Technology Research Journal*, 16(4), 201-210. <https://doi.org/10.12913/22998624/152790>
12. Mandel. Definition of a suitable frame for the study of anelastic transformations of the polycrystal. *J Mec Appl*. 1982; 1: 7-23.
13. Dafalias Y. Plastic spin concept and a simple illustration of its role in finite plastic transformations. *Mechanics of Materials*, 1988; 3: 223-233, [https://doi.org/10.1016/0167-6636\(84\)90021-8](https://doi.org/10.1016/0167-6636(84)90021-8)
14. Sidoroff F, Teodosiu C. Microstructure and Phenomenological Models for Metals. *Large Deformations of Solids: Physical Basis and Mathematical Modelling*, 1986. https://doi.org/10.1007/978-94-009-3407-8_11.
15. Dogui A. Two-dimensional kinematics in large deformations; application to off-axis traction and torsion. *Journal of theoretical and applied mechanics*. 1988; 7(1): 43-64.
16. Zhani K, Darrieulat M, Chenaoui. Prediction of single crystal instability in channel-die compression using Rice's criterion. *J Braz Soc Mech Sci Eng*. 2022; 44: 308. <https://doi.org/10.1007/s40430-022-03610-y>
17. Zhani K, Darrieulat M, Chenaoui A. Prediction of Anisotropic Elastoplastic Instability with Rice's Criterion in Plane Compression. *Indian Journal of Science and Technology*. 2021; 14(18): 1452-67. <https://doi.org/10.17485/IJST/v14i18.117>
18. Rice JR. Theoretical and applied mechanics. In: *Proc of the 14th IUTAM Congress, North-Holland*. Amsterdam, Netherlands; 1976: 207-220.
19. Ladeveze P. On the theory of plasticity in large deformations. Internal Report, 1980; 9.
20. Cordebois. Plastic instability criterion and ductile damage in large deformations. 1983.
21. Sidoroff F. Phenomenological models. Oleron summer school: physics and mechanics of metal

- shaping, directed by F. moussy and P. franciosi. In: CNRS / IRDID presses. Paris 1990: 299-310,
22. Habbad M, Sidoroff F. Application of the Swift instability criterion to some anisotropic models. In: Proceedings of the 1st Congress of Mechanics organised by the Moroccan Society of Mechanical Sciences. Rabat: Morocco; 75-82.
 23. Dogui A. Anisotropic plasticity undergoing major transformations. PhD Thesis (in French). University Claude Bernard Lyon I; 1989.
 24. Sidoroff F, Dogui A. Some issues about anisotropic elastic-plastic models at finite strain. *International Journal of Solids and Structures*, 2001; 38: 9569-957. [https://doi.org/10.1016/S0020-7683\(01\)00139-1](https://doi.org/10.1016/S0020-7683(01)00139-1)
 25. Mandel J. Constitutive equations and directors in plastic and viscoplastic materials. *International Journal of Solids and Structures*. 1973; 9(6): 725-40. [https://doi.org/10.1016/0020-7683\(73\)90120-0](https://doi.org/10.1016/0020-7683(73)90120-0).
 26. Saadi N, Zhani K, Fethallah K, Chenaoui A, Dkiouak R. Curve Limit of Formation for the Isotropic Plasticity. In: Ezziyyani M, editor. *Advanced Intelligent Systems for Sustainable Development (AI2SD'2019)* AI2SD 2019 Advances in Intelligent Systems and Computing. Cham: Springer; 2020. https://doi.org/10.1007/978-3-030-36671-1_17
 27. Hill R. *Theoretical plasticity of textured aggregates*. math, Proc, Cam. 1990.
 28. Storen S, Rice JR. Localized necking in thin sheet. *Journal of the Mechanics and Physics of Solids*, 1975, 23(6): 421-41.
 29. Habraken AM, Duchêne L. Anisotropic elasto-plastic finite element analysis using a stress-strain interpolation method based on a polycrystalline model. *International Journal of Plasticity* 2004; 20(8-9): 1525–1560. <https://dx.doi.org/10.1016/j.ijplas.2003.11.006>.
 30. Abu Shaban, N., Al-Qawabah, S. M., Alkhaldi, H. S. (2023). Investigation of Multi-Cold Rolling Passes on Mechanical Characteristics and Surface Quality of AlCuV Alloy. *Advances in Science and Technology Research Journal*, 17(5), 68-76. <https://doi.org/10.12913/22998624/171265>
 31. Poussardin. Characterization and evolution of shear bands in Al-Mn single crystals of different crystallographic orientations. PhD Thesis (in French), 2003.